Rheologica Acta (2021) 60:209–218
https://doi.org/10.1007/s00397-021-01263-7

ORIGINAL CONTRIBUTION

Graphene oxide dispersion state in polystyrene-based composites below percolation threshold via linear melt rheology

Claudia Dessi[1] · Leice G. Amurin[2,3] · Pablo A. R. Muñoz[1] · Yuri D. C. de Oliveira[1] · Guilhermino J. M. Fechine[1] · Ricardo J. E. Andrade[1]

Received: 30 June 2020 / Revised: 30 November 2020 / Accepted: 8 February 2021 / Published online: 6 March 2021

Abstract

In this work, the relation between the morphological structure and the linear viscoelasticity of graphene oxide (GO)-based polystyrene nanocomposites below percolation threshold was investigated. The rheological properties were observed to change upon addition of GO-2D particles at filler content below mechanical percolation threshold (0.06–0.3 %vol). In particular, the nanocomposite systems showed a delayed long-range relaxation dynamic regardless particle concentration, when compared to the neat polystyrene matrix. Moreover, little shift with regard to higher relaxation times of the full relaxation spectra of PS-GO nanocomposite was observed. This is attributed to the presence of attractive-kind interfacial interaction between polymer chains and GO-2D particles via π-π binding of benzyl rings, which strongly depends on GO sheets dispersion and exfoliation state. In light of these observations, oscillatory shear rheology measurements were used as an indirect tool to establish how exfoliated GO-2D particles were homogeneously dispersed in a low-polar polymer matrix.

Keywords 2D particles · Graphene oxide · Polymer nanocomposites · Linear viscoelasticity · Time-temperature superposition principle · Relaxation time spectrum · Attractive interfacial interactions

Introduction

After being successfully isolated in 2004 by Novoselov et al. (Novoselov et al. 2004), graphene became one of the most promising two-dimensional (2D) material, due to its unique thermal, electrical, and mechanical properties (Stankovich et al. 2006; Kuilla et al. 2010). The recent advances in graphene mass production enabled high-rate manufacturing of new graphene-based materials as well, suitable for the next generation of polymer nanocomposites (Mittal 2014; Saravanan et al. 2014). In particular, graphene oxide (GO) has become one of the most popular due to its straightforward synthesis from graphite oxide by exfoliation sonication in water (Hummers and Offeman 1958; Dreyer et al. 2010; Chen et al. 2013) and its large potential of application in many different fields (Zhu et al. 2010).

Final composite properties highly depend on homogeneous and fine dispersion of the filler phase into the hosting matrix. Various processing techniques of polymer nanocomposites have been recently reviewed where the role of processing conditions, surface chemistry/modification of fillers, and polymer-filler compatibility is probed in order to achieve good filler dispersion in the first place (Fawaz and Mittal 2014). Earlier studies have reported several combinations of melt intercalation and extrusion technique for polymer composites compounding with graphene-based 2D particles, where different final dispersion states are obtained depending on the actual particle exfoliation efficiency, i.e., 2D particle aspect ratio (Kim et al. 2010a; El Achaby et al. 2012; Munoz et al. 2018). Although using pre-exfoliated 2D particles generally represents the main key-factor to obtain a good filler dispersion, graphene-based-polymer nanocomposite morphology and its viscoelastic behavior are shown to be significantly

Claudia Dessi and Leice G. Amurin contributed equally to this work.

✉ Ricardo J. E. Andrade
ricardo.andrade@mackenzie.br

[1] Department of Physics, Georgetown University, 3700 O Street NW, Washington, DC 20057, USA

[2] Mackgraphe - Mackenzie Institute for Research in Graphene and Nanotechnologies, Instituto Presbiteriano Mackenzie-SP, Rua da Consolação 896, São Paulo, SP 01302-907, Brazil

[3] Center of Technology in Nanomaterials (CTNano) at Federal University of Minas Gerais (UFMG), Belo Horizonte, Minas Gerais, Brazil

affected by initial particle concentration and processing parameters, such as extrusion screw rotational speed (Munoz et al. 2018), deformation history, and annealing time (Kim and Macosko 2009).

GO have recently attracted a lot of interest in both research and industry field since they have been shown to have broad intermolecular interactions with many types of polymeric systems (Kuilla et al. 2010; Potts et al. 2011; Hu et al. 2014; de Oliveira et al. 2019b) due to their size-dependent amphiphilicity (Kim et al. 2010b). Indeed, GO-polymer nanocomposites are generally characterized by good particle dispersion degree, high interfacial adhesion strength, and reinforcement efficiency due to electrostatic and van der Waals intermolecular forces, even in low-polar polymer systems (Wan and Chen 2012). Moreover, it has been shown as well that GO can act as "processing aids" in different polymeric matrices, allowing to produce high performance materials with less severe processing parameters and with very low concentrations (Pinto et al. 2020; Danda et al. 2020).

A universal description of polymer nanocomposites and their viscoelastic properties is still missing due to the variable nature of both particle phase and particle-polymer interactions. However, many carbon-based composites have showed a characteristic viscoelastic response in terms of storage modulus at low frequency, creep-recovery compliance, and shear thinning exponent typical of other filled systems at percolation and above-percolation filler concentrations (Zhao et al. 2005; Leblanc 2009; Münstedt 2016; Ivanov et al. 2017). Rheological percolation concentration has indeed been used as particle dispersion indicator in many polymer composite systems for the observed mechanical reinforcement and viscosity increase (Wagener and Reisinger 2003), with a strong correlation to electrical percolation in some cases (Pötschke et al. 2002; Wu et al. 2006; Chen et al. 2015; Helal et al. 2019). In case of anisotropic particles, percolation-threshold concentrations are found to be inversely proportional to the aspect ratio and the dispersion state of particles, mainly explained via excluded volume theory (Balberg et al. 1984; Garboczi et al. 1995; Kharchenko et al. 2004; Stankovich et al. 2006; Li et al. 2007; Sun et al. 2009; Nan et al. 2010; Stauffer et al. 2014). Moreover, different polymer-filler blending methods (Ivanov et al. 2017), and bulk polymer architecture (Liao et al. 2012) are shown to significantly affect percolation-threshold as well.

Besides mechanical reinforcement effects and viscosity increase expected upon particles addition, reduction of shear modulus and viscosity have been also reported for spherical and platelet particles (Mackay et al. 2003; Zhang et al. 2006; Jain et al. 2008; Munoz et al. 2018; de Oliveira et al. 2019b; Ferreira et al. 2019). Such viscoelastic response has been addressed via nanoparticles confinement (Mackay et al. 2003), and selective polymer chain adsorption (Zhang et al. 2006; Jain et al. 2008), or stack interlayer slipping (Song et al. 2014; Munoz et al. 2018; de Oliveira et al. 2019b) for polymer composites prepared from either solution blending or melt compounding. Ferreira et al. have recently suggested that aggregate-aggregate slippage is more likely to occur when modulus and viscosity decrease are observed under shear deformations for molten graphene-based nanocomposites due to the incommensurable contact of the high stack interlayer of graphite, graphite oxide, and graphene oxide platelets (Ferreira et al. 2019).

Although nanocomposite properties are mainly determined by particle network when particle content is above percolation-threshold, 2D-particle composites represent an intriguing category of materials to exploit relations between the microscopic mechanism and macroscopic rheology at below percolation-threshold as well, due to their enhanced specific area and interphase interactions. To this end, viscoelasticity of polymer nanocomposites can be probed in the linear regime in more details without incurring in well-known problems associated with composite melt rheometry, such as time-temperature equivalence (Zouari et al. 2012), and wall slip over solid surfaces (Malkin 1990; Leblanc 2002).

To the best of our knowledge, no attempt has been made so far to investigate the relation between the morphological dispersion and the rheological behavior/response of GO-polymer nanocomposites at filler content below percolation-threshold. Based on our recent results on successful two novel melt compounding strategies for polymer nanocomposites with low agglomeration concentration of GO and other 2D particles (Munoz et al. 2018), the present work reports the rheological signature of GO-polystyrene nanocomposites at particle concentration below percolation-threshold obtained via liquid-phase feeding (LPF) method as described elsewhere (Munoz et al. 2018). The nanocomposite morphology was analyzed via scanning electron microscopy and X-ray microtomography, showing different levels of dispersion and exfoliation of GO within the matrix. The linear viscoelastic behavior is investigated via dynamic oscillatory measurements, where time-temperature superposition principle is analyzed, and shows long-range dynamics only to be affected depending on the dispersion and exfoliation degree of GO particles, as confirmed by relaxation spectra.

Materials and methods

Materials

Homopolymer polystyrene (PS) (ρ = 1.05 g cm^{-3}, M_w = 170600 g mol^{-1}, and PI ~ 2) was provided by INOVA, Brazil. Natural graphite powder (≤ 150 μm, 99.9%) was purchased from Sigma-Aldrich. Potassium permanganate ($KMnO_4$, 99%) was purchased from Sigma-Aldrich. Sulfuric acid ($H2_SO_4$ 98%), hydrochloric acid (HCl, 6 M), hydrogen

peroxide (H_2O_2, 30% v), and ethanol ACS were supplied by Vetec. All the materials were used as received.

Synthesis of multilayer graphene oxide

Graphite oxide (GrO) was prepared from powdered flake graphite following Hummer´s modified method (Hummers and Offeman 1958; Stankovich et al. 2007) by decreasing the total oxidation time to one hour as described in our previous study (Munoz et al. 2018). Pre-exfoliated graphene oxide (GO) 2D particles were obtained by adding GrO (200 mg) to 100 mL of deionized water, then sonicated for 30 min. Final GO suspensions were constantly stirred at ~ 350 rpm in order to avoid earlier precipitation before their incorporation into the polymer matrix. The obtained material presented most of the particles around 17 nm thickness (< 20 layers), and lateral size about 400 nm, as described in our previous work (Munoz et al. 2018).

Preparation of graphene oxide-based polystyrene nanocomposites

The filler-polymer mixing did occur in a co-rotational twin-screw extruder with length-to-diameter (L/D) ratio = 40 with constant rotation speed of 350 rpm (Process 11, ThermoScientific). The polymer was fed to the extruder at a constant mass rate of 4 g min^{-1}, whereas the GO suspension was injected via a peristaltic pump system. The extruder operational temperature ranges from hopper to die was as follows: 170 / 230 / 250 / 250 / 260 / 230 °C. In this way, GO particles were always added at the polymer flow state above glass transition temperature T_g for polystyrene, enhancing filler-polymer mixing. The final filler concentrations of the polymer nanocomposite investigated in this work were controlled via peristaltic pump flow rate and were equal to 0.06, 0.18, and 0.3 vol% via liquid-phase feeding (LPF) method. More details about filler-polymer extrusion processing can be found in Munoz et al.'s work (Munoz et al. 2018).

Characterization methods

Computerized micro-tomography

X-ray microtomography samples with 8 mm^3 from tensile strength specimens were used and analyzed in a SkyScanner 1272 (Bruker). A 20-kV and 175-μA source was used with 2 μm/pixel resolution.

Scanning electron microscopy

To examine the GO particle dispersion and size, the samples were cut into ultrathin slices (~ 60 nm thick) using a Leica model CM 1850 series microtome at room temperature. Then, the samples were observed in a Jeol JSM-7800F microscopy in transmission mode at 30 keV equipped with an energy filter spectrometer within the column.

Rheology

Viscoelastic behavior of GO nanocomposites was investigated by a series of dynamic oscillatory in shear with a controlled stress rheometer (Anton Paar, Physical MCR 102) equipped with stainless steel 25 mm diameter parallel plate geometry/measuring system and a Peltier bath as temperature control unit. Disk specimens with 25 mm diameter and 1 mm thickness were prepared by applying ~ 17 bars (3 tons-force) for 2 min at 230 °C in a hot press. The specimens were allowed to relax for 5 min in order to release any residual stress developed during the compression molding process before performing any rheological measurement. Fresh sample was loaded at each operational temperature and good contact between the sample and the plates was ensured with careful normal force monitoring. Oscillatory shear measurements were carried out at 1 mm gap and at three different temperatures (180, 200, and 230 °C) under nitrogen air atmosphere (> 99% nitrogen purity at 5 bar from manufacture instructions) to avoid sample degradation. In order to determine the linear viscoelastic region of GO nanocomposites, strain sweep tests were performed applying shear strain values from 0.1 to 100% and at angular frequencies of 0.1, 10, and 100 rad/s (results not shown here).

From frequency sweep tests, dynamic moduli G' and G" (storage and loss modulus, respectively) were measured as a function of angular frequency ω (100–0.01 rad/s) at strain values between 0.5 and 10% according to the linear material response window during the strain sweep test.

Results and discussion

Graphene oxide composites morphology

Information about GO characterization can be found in our previous study (Munoz et al. 2018). Here, we present the morphological information obtained by micro-CT that shows GO segregation in all compositions, even at the lowest GO concentration (0.06 vol%) (see Fig. 1a and b). The main difference between the two samples is the number of particles. Munoz et al. reported 113 particles/mm^3 and 384 particles/mm^3 for samples 0.06 vol% and 0.30 vol%, respectively. No significative geometrical changes were noticed between phases within the different PS-GO composites as observed by superficial area distribution in Fig. 1c. The fact that no change is observed in particles sizes may indicate that our filler-polymer processing induces the segregated morphology, probably because of the combination of fast evaporation of

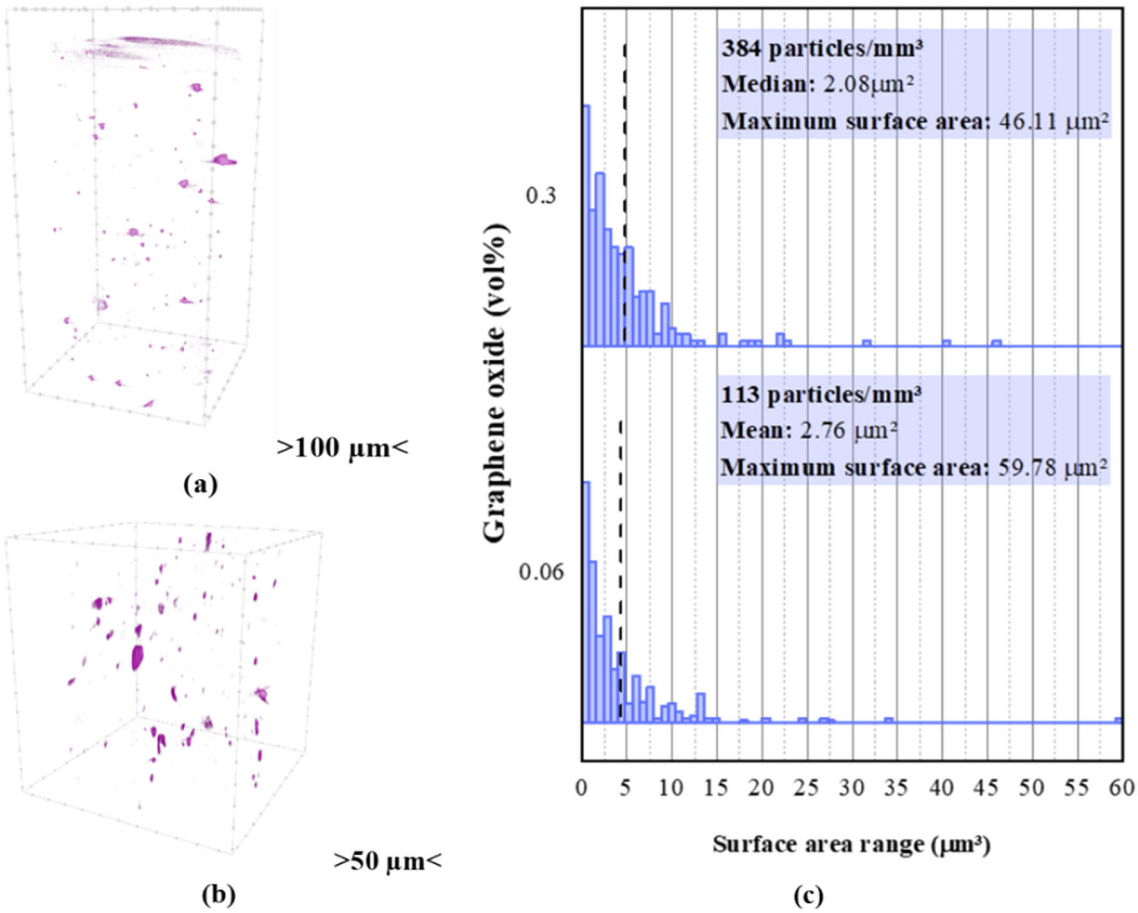

Fig. 1 Reconstructed micro CT images of PS composites with (**a**) 0.06 vol%, (**b**) and 0.30 vol% of GO; (**c**) Superficial area distribution estimate using CTAn and CTVol softwares, images generated in CTVox (Brüker)

water molecules in contact with softened polymer and low compatibility between filler and polymer phases.

Due to the presence of oxygenated groups, GO presents an excellent colloidal stability in water, mainly attributed to ionizable edge-COOH groups (Lerf et al. 1998; Li et al. 2008). These functional groups are located at a basal plane made of hydrophobic unoxidized benzene rings (Nakajima and Matsuo 1994; Cai et al. 2008), which confers an amphiphilic nature to GO. Due to this nature, GO particles has been demonstrated to be edge-to-area ratio dependent (Cote et al. 2009; Kim et al. 2010a). As well as GO particles, PS chains present aromatic rings along their backbone chain, being able to establish secondary weak forces, mainly π-π interactions. Yang et al. indeed observed that PS chains and GO particles show intermolecular interactions via π-π conjugation, where the phenyl groups of PS side chains tend to be vertical to the surface of graphene-based sheets (Yang et al. 2005). On the other hand, GO particles can interact among them through their graphene-based basal plane and oxygenated basal-edge groups due to π-π interactions and short-range electrostatic interactions (such as van der Waals forces), respectively. The GO-GO interaction is somewhat dominant and reduces the possibility of GO dispersion into PS matrix at nanometric scale, keeping microphase stable, even after GO particles pre-exfoliation, as observed in micro CT images in Fig. 1a and b. Since we demonstrated no geometrical differences between the phases of PS and GO within composites with 0.06 vol% and 0.30 vol%, the effect of GO in the composite final properties is a consequence of the number of particles per volume unit only, that changes the total available interfacial area.

The morphological dispersion features of the 2D GO particles in the polymer matrix were observed by scanning electron microscopy (SEM). Figure 2a and b show the SEM micrographs of the PS-GO nanocomposites samples with 0.06 vol% and 0.30 vol%. The GO particles can be readily recognized from the observation in contrast difference, with respect to the polymer matrix, from which the shape and the size of the exfoliated and dispersed 2D GO particles are observed by SEM images. The thin GO layers observed in Fig. 2a indicate high degree of exfoliation. Figure 2b displays the increase of segregation with the concentration of the PS-GO nanocomposites samples with 0.30 vol%; however, it is still possible to observe thin layers indicating the exfoliated state of the GO layers inside the matrix.

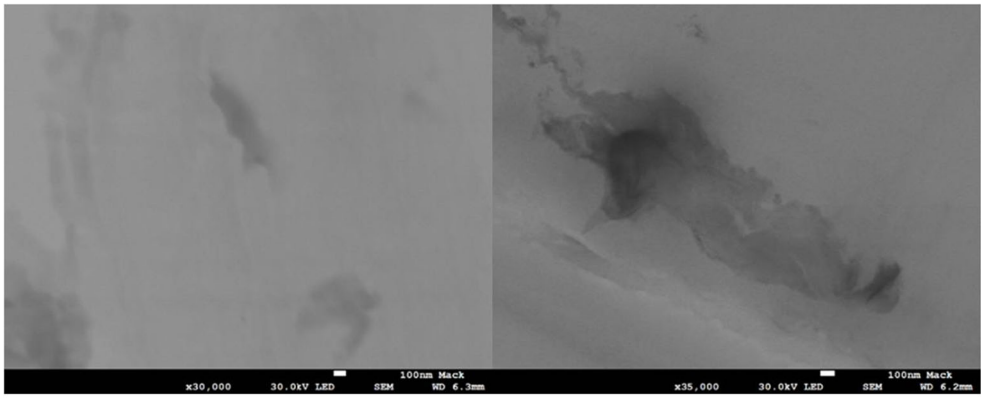

Fig. 2 Scanning electron micrographs of PS composites with (**a**) 0.06 vol%, and (**b**) 0.30 vol% of GO

Linear viscoelasticity behavior

Polymer nanocomposites obtained via polymer-filler melt blending have their mechanical properties directly related to the dispersion state of particles and polymer-particle interactions (Lebaron et al. 1999; Ding et al. 2005; de Oliveira et al. 2019a). It is therefore very important to be able to quantify size and dispersion degree of the particles embedded into the polymeric matrix. To this end, we have performed a series of small amplitude oscillatory shear measurements at three different temperatures on our PS-based nanocomposites filled with GO-2D particles at different volume concentrations.

Figure 3 displays the evolution of storage (G') and loss (G") moduli as a function of frequency for both neat PS matrix and PS-GO nanocomposites. Specifically, both dynamic moduli are presented as master curves at T_{ref} = 200 °C and obtained by frequency-scale a_T shifts only as time-temperature dependence. The observed mechanical spectrum for all the systems describes the terminal relaxation behavior upon reaching the terminal crossover within the displayed frequency range. In particular, a typical viscoelastic liquid scaling for the terminal relaxation region (i.e., G" ∝ ω and G' ∝ ω^2) is observed for both neat PS matrix and all PS-GO nanocomposites. The terminal relaxation time λ, corresponding to the inverse of the terminal crossover frequency, is found to shift towards higher values for PS-GO nanocomposites with respect to the neat PS matrix but independent of filler concentration (λ_{PS} ~ 6 ms for neat PS matrix, $\lambda_{PS\text{-}GO}$ ~ 10 ms for all nanocomposites).

These findings suggest that GO-2D particles are capable to engage and slow down the entanglement relaxation process of linear PS chains within the polymer matrix, independently on the volume concentration of particles investigated. Similar behavior was observed in solid state through low-field nuclear magnetic resonance (Munoz et al. 2018). This is a little in contrast to what observed for other anisotropic graphene-

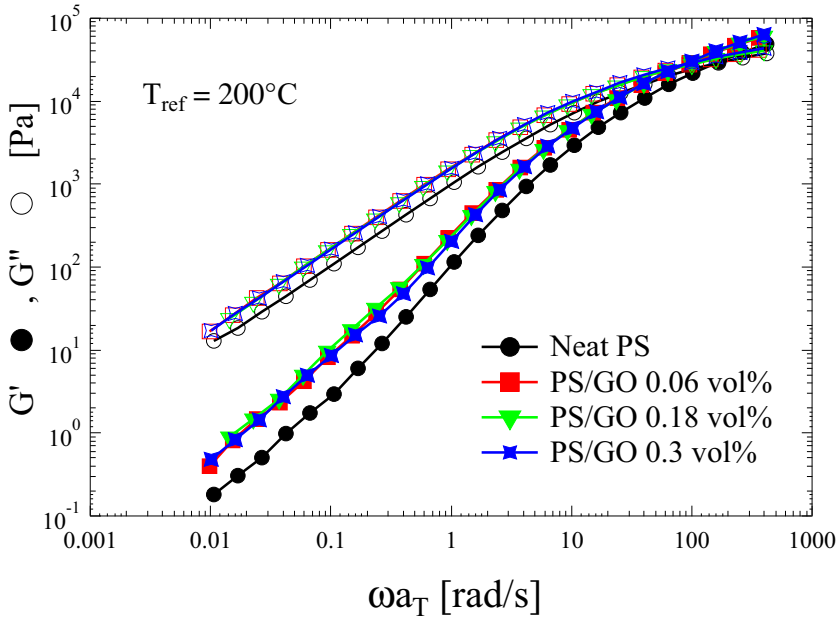

Fig. 3 Master curves of storage (G') and loss (G") modulus as function of reduced angular frequency (ωa_T) at T_{ref} = 200 °C for neat polystyrene (PS) and its graphene oxide-based nanocomposites (PS-GO) at three different volume concentrations for particles content

based polymer composites, in particular carbon nanotubes-filled systems, where the small strain dynamic properties suggest high memory behavior already at particle concentration values as small as our case study (Kharchenko et al. 2004; Du et al. 2004). On the other hand, the temperature dependence of experimentally observed relaxation times is seen to follow the well-known WLF dependence for all the investigated systems (Ferry 1980),

$$\log a_T = \frac{-C_1^0(T-T_0)}{C_2^0 + T - T_0} \quad (1)$$

where a_T is the frequency-scale shift, T and T_0 are the experimental and reference temperature, respectively, C_1^0 and C_2^0 are the fitting parameters at the reference temperature. Figure 4 shows experimental data of log a_T as a function of temperature for both neat PS matrix and PS-GO nanocomposites at reference temperature $T_0 = 200$ °C, which were fitted by using Eq. 1. Values of C_1^0 and C_2^0 parameters are within the range of the PS matrix for all the systems and are confirmed by previous experimental observations for linear PS at the same reference temperature (Coppola 2020, private communication). This confirms that experimentally observed relaxation times of both neat PS matrix and PS-GO nanocomposites have the same temperature dependence. Thus, local microstructure of linear PS chains is not altered by the presence of GO-2D particles at the investigated volume concentrations.

No significant mechanical reinforcement via modulus increase is observed at frequencies higher than the terminal crossover between PS-GO nanocomposites and PS matrix. Therefore, while hindering polymer chains motion within their reptation tube, GO-2D particles do not form a fully percolated filler network, even at the highest particle content (0.3 vol%). This is in contrast with what recently observed for GO aqueous suspensions (Ng et al. 2020) and other polymeric media (Gudarzi and Sharif 2012). On the other hand, our finding is in line with earlier results reporting percolation threshold starting at ~ 0.5–0.6 %vol when filler-polymer melt compounding without sonication was employed (Kim and Macosko 2009).

Influence of GO particles size on chain molecular relaxation

In the linear theory of viscoelastic fluids, relaxation time spectrum $H(\tau)$ is an efficient tool to probe the effects of polymer-filler interface on local and/or global relaxation dynamics of polymer molecules when experimental linear viscoelastic material functions are available (Kotsilkova and Pissis 2007; Angelov et al. 2014).

The relaxation time spectrum $H(\tau)$ is referred as the set of contributions of relaxation processes occurring within the sample. Each relaxation process provides a strength at certain time scale to the overall relaxation process of polymer chains. As particles are added, in case the mobility of polymer chains

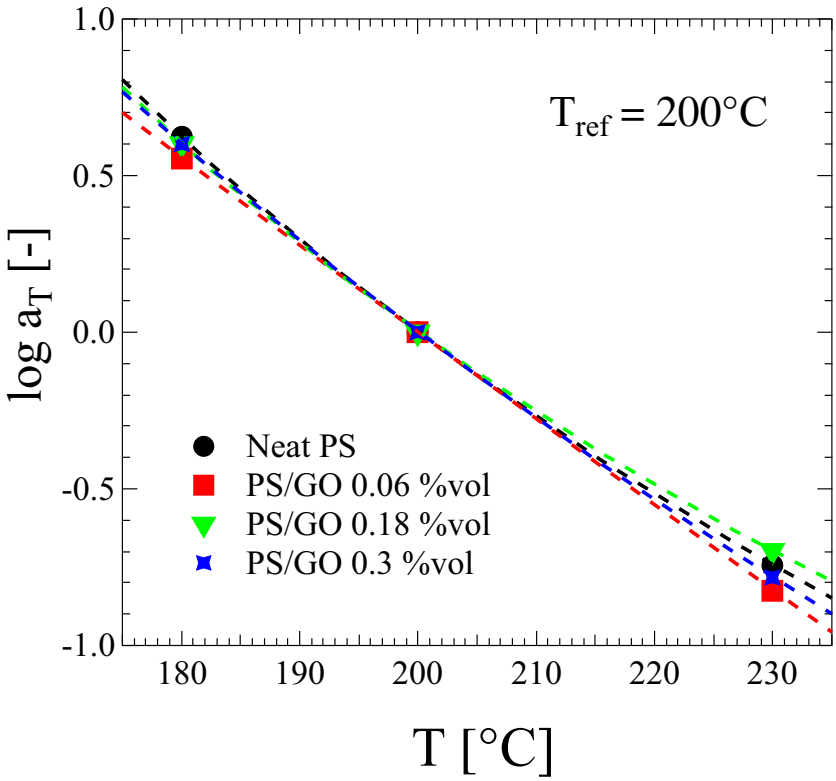

Fig. 4 Experimental data of log a_T as a function of temperature for both neat PS matrix and PS-GO nanocomposites at reference temperature $T_{ref} = 200$ °C (full symbol), along with WLF temperature dependence fitting curves by using Eq. 1 (dashed line)

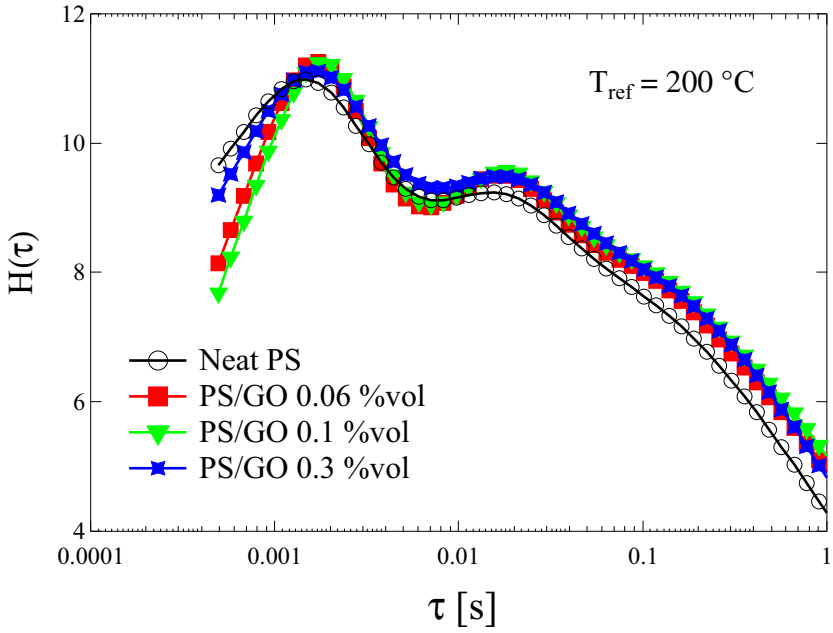

Fig. 5 Relaxation spectrum $H(\tau)$ as a function of relaxation time τ for neat PS matrix and PS-GO nanocomposites at T_{ref} = 200 °C

is affected, the relaxation time spectrum can either shift or broaden (i.e., global or local changes in polymer relaxation behavior, respectively) due to polymer-filler interface effects (Sternstein and Zhu 2002; Angelov et al. 2014).

Figure 5 displays the relaxation time spectrum $H(\tau)$ as a function of relaxation time τ which was calculated by using the program ReSpect v2.0 developed by Takeh and Shanbhang (Takeh and Shanbhag 2013). A little shift of the full relaxation spectra of PS-GO nanocomposite towards higher relaxation times compared to the neat PS matrix is observed, but no appreciable broadening as well. This confirms our earlier results on dynamic moduli where the relaxation dynamics on the

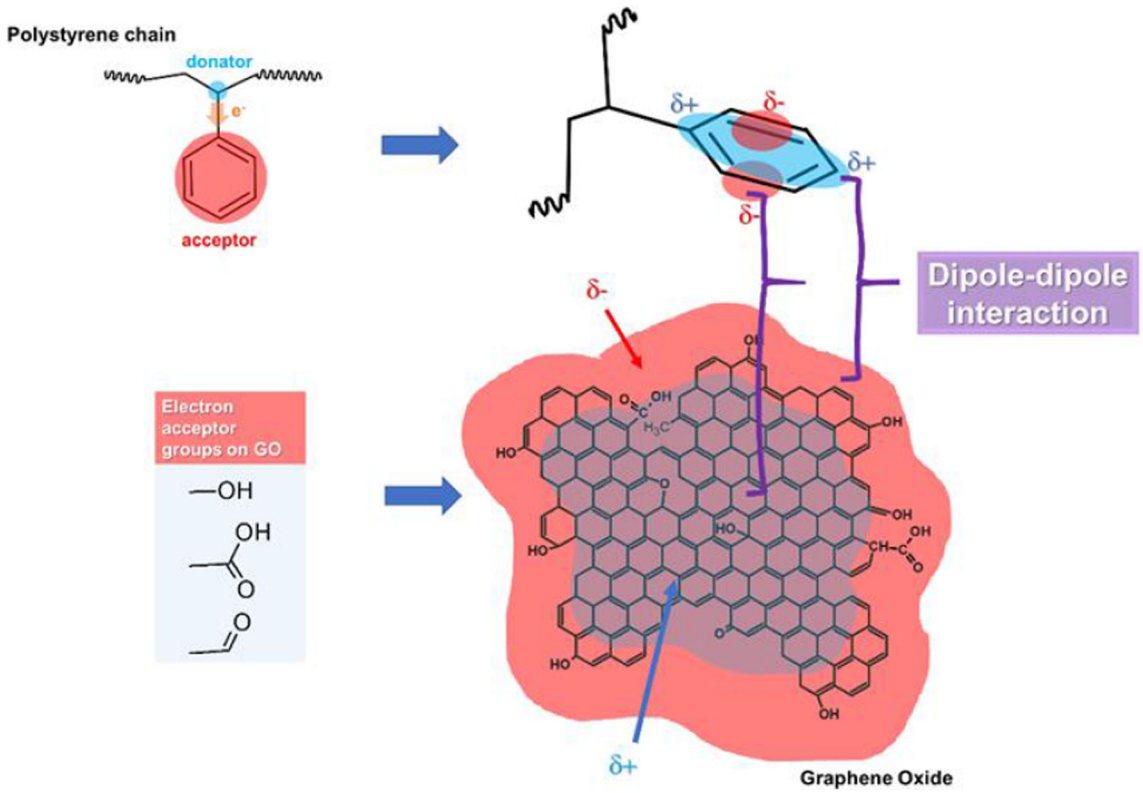

Fig. 6 Schematic of the expected interactions between polystyrene chains and GO

whole linear polymer chain only (e.g., reptation) are observed to be affected upon GO-2D particles addition to the polymer host, but no significative change in the local polymer relaxation behavior (i.e., same temperature dependence). It is worth mentioning that, given its small intensity, the presence of a second peak in the relaxation spectrum of all the systems is attributed to some polydispersity of linear PS chains, which further broadens the observed spectrum (Ferry 1980).

Ellison et al. showed that for amorphous polymers, the presence of attractive interfaces could decrease the mobility of the whole polymer chain, whereas repulsive interfaces can increase the molecular mobility (Ellison and Torkelson 2003). Apparently, the presence of GO-2D particles in PS matrix directly affects the terminal relaxation time of the polymer chains by means of attractive particle-polymer interfaces. They act as an energetic barrier for the motions of at least several Kuhn length of the polymer chain segments that are in direct contact to the particle surface. As seen for carbon nanotubes and other graphene-based sheets composite materials (Yang et al. 2005), such attractive polymer-particle interactions have been addressed as π-π conjugation between the side phenyl groups of linear PS chains and graphene-based basal plane of GO-2D particles. These attractive π-π interactions are due to the electronic displacements in aromatic ring, caused by lateral group, which generates a quadripole as proposed by Martinez and Iverson (Martinez and Iverson 2012). This electronic displacement takes place in phenyl groups located at PS chain and graphene-based basal plane of GO as displayed in Fig. 6. Due the electrostatic attraction between the quadripoles, the phenyl groups of PS tend to stack with GO graphitic plane through the alignment of opposite poles. GO with different oxidation levels have already been demonstrated that influences the rheological behavior of different systems (Soares et al. 2020; Moraes et al. 2020). Thus, as a future work, different oxidation degrees of GO should be studied with the aim to investigate how it will change the electronic displacement by tuning the interphase interactions development.

Moreover, a clear signature of percolation and network induction of graphene particles is missing, confirming the hypothesis/speculation that only particle-polymer interactions can take place within the polymer matrix as long as attractive-like particles are homogeneous dispersed at below-percolation concentration.

Conclusions

In this work, the melt linear viscoelastic properties of PS-GO nanocomposites under oscillatory shear were investigated and correlated with the morphological information obtained by micro-CT and SEM. Comparison of the dynamics moduli (G' and G") in the frequency domain between the linear neat polymer matrix and nanocomposites reveals only long-range dynamics perturbations when GO-2D particles content is below percolation threshold. Indeed, the presence of particles extends the reptation dynamics effect of the linear PS chains towards higher relaxation times, regardless the particle content, while the moduli response did not show any apparent mechanical reinforcement effect. Our hypothesis is that attractive interfacial interactions between polymer chains and GO-2D particles via π-π binding of benzene rings are causing the stress tube relaxation delay of each linear PS chain, as seen for other graphene-based polymer nanocomposites. Taking into account that such attractive interactions depend on GO exfoliation level, our findings in oscillatory shear rheology are an indirect evidence of high exfoliated GO-2D particles homogeneously embedded into PS-GO nanocomposites. Given the low particle concentration range exploited in this case study, we ensured that flow properties of PS-GO nanocomposites were not affected by the superposition of particle-particle interactions due to percolated filler network.

Moreover, a good processing of such polymer composite systems is easy to achieve at different production scales, with graphene content fulfilling other requested material properties (e.g., electrostatic discharge), which requires only a relatively low level of concentration.

Acknowledgements The authors thank INOVA, Brazil, for the supply of materials.

Funding This study received funding from Fundação de Amparo a Pesquisa de São Paulo (FAPESP) under grants 2012/50259-8, 2014/22840-3, 2016/12400-1, 2017/07244-3, and 2018/10910-8. This work was also partially funded by Fundo Mackenzie de Pesquisa (MackPesquisa, Project Number 181009), Conselho Nacional de Desenvolvimento Científico e Tecnológico (CNPq, Finance code 001), and Coordenação de Aperfeiçoamento de Pessoal de Nível Superior (CAPES) - PRINT 88887.310339/2018-00. G.J.M.F. received financial support from CNPq (grant 307665/2018-6) and Laboratório Nacional de Nanotecnologia (LNNano, Project Number Micro CT-23259) for the computerized micro-tomography measurements.

Declarations

Conflict of interest The authors declare no competing interests.

References

Angelov V, Velichkova H, Ivanov E, Kotsilkova R, Delville MH, Cangiotti M, Fattori A, Ottaviani MF (2014) EPR and rheological study of hybrid interfaces in gold-clay-epoxy nanocomposites. Langmuir 30:13411–13421. https://doi.org/10.1021/la503361k

Balberg I, Anderson CH, Alexander S, Wagner N (1984) Excluded volume and its relation to the onset of percolation. Phys Rev B 30: 3933–3943. https://doi.org/10.1103/PhysRevB.30.3933

Cai W, Piner RD, Stadermann FJ et al (2008) Synthesis and solid-state NMR structural characterization of 13C-labeled graphite oxide. Science (80-) 321:1815–1817. https://doi.org/10.1126/science.1162369

Chen J, Yao B, Li C, Shi G (2013) An improved Hummers method for eco-friendly synthesis of graphene oxide. Carbon N Y 64:225–229. https://doi.org/10.1016/j.carbon.2013.07.055

Chen Q, Gong S, Moll J, Zhao D, Kumar SK, Colby RH (2015) Mechanical reinforcement of polymer nanocomposites from percolation of a nanoparticle network. ACS Macro Lett 4:398–402. https://doi.org/10.1021/acsmacrolett.5b00002

Cote LJ, Kim F, Huang J (2009) Langmuir-blodgett assembly of graphite oxide single layers. J Am Chem Soc 131:1043–1049. https://doi.org/10.1021/ja806262m

Danda C, Amurin LG, Muñoz PAR, Nagaoka DA, Schneider T, Troxell B, Khani S, Domingues SH, Andrade RJE, Fechine GJM, Maia JM (2020) Integrated computational and experimental design of ductile, abrasion-resistant thermoplastic polyurethane/graphene oxide nanocomposites. ACS Appl Nano Mater 3:9694–9705. https://doi.org/10.1021/acsanm.0c01740

de Oliveira CFP, Muñoz PAR, dos Santos MCC, Medeiros GS, Simionato A, Nagaoka DA, de Souza EAT, Domingues SH, Fechine GJM (2019a) Tuning of surface properties of poly(vinyl alcohol)/graphene oxide nanocomposites. Polym Compos 40: E312–E320. https://doi.org/10.1002/pc.24659

de Oliveira YDC, Amurin LG, Valim FCF, Fechine GJM, Andrade RJE (2019b) The role of physical structure and morphology on the photodegradation behaviour of polypropylene-graphene oxide nanocomposites. Polymer (Guildf) 176:146–158. https://doi.org/10.1016/j.polymer.2019.05.029

Ding C, Jia D, He H, Guo B, Hong H (2005) How organo-montmorillonite truly affects the structure and properties of polypropylene. Polym Test 24:94–100. https://doi.org/10.1016/j.polymertesting.2004.06.005

Dreyer DR, Park S, Bielawski CW, Ruoff RS (2010) The chemistry of graphene oxide. Chem Soc Rev 39:228–240. https://doi.org/10.1039/B917103G

Du F, Scogna RC, Zhou W et al (2004) Nanotube networks in polymer nanocomposites: rheology and electrical conductivity. Macromolecules 37:9048–9055. https://doi.org/10.1021/ma049164g

El Achaby M, Arrakhiz F-E, Vaudreuil S et al (2012) Mechanical, thermal, and rheological properties of graphene-based polypropylene nanocomposites prepared by melt mixing. Polym Compos 33: 733–744. https://doi.org/10.1002/pc.22198

Ellison CJ, Torkelson JM (2003) The distribution of glass-transition temperatures in nanoscopically confined glass formers. Nat Mater 2: 695–700. https://doi.org/10.1038/nmat980

Fawaz J, Mittal V (2014) Synthesis of polymer nanocomposites: review of various techniques. In: Synthesis techniques for polymer nanocomposites. Wiley-VCH Verlag GmbH & Co. KGaA, Weinheim, pp 1–30

Ferreira EHC, Andrade RJE, Fechine GJM (2019) The "superlubricity state" of carbonaceous fillers on polyethylene-based composites in a molten state. Macromolecules 52:9620–9631. https://doi.org/10.1021/acs.macromol.9b01746

Ferry JD (1980) Viscoelastic properties of polymers. Wiley

Garboczi EJ, Snyder KA, Douglas JF, Thorpe MF (1995) Geometrical percolation threshold of overlapping ellipsoids. Phys Rev E 52:819–828. https://doi.org/10.1103/PhysRevE.52.819

Gudarzi MM, Sharif F (2012) Enhancement of dispersion and bonding of graphene-polymer through wet transfer of functionalized graphene oxide. Express Polym Lett 6:1017–1031. https://doi.org/10.3144/expresspolymlett.2012.107

Helal E, Kurusu RS, Moghimian N, Gutierrez G, David E, Demarquette NR (2019) Correlation between morphology, rheological behavior, and electrical behavior of conductive cocontinuous LLDPE/EVA blends containing commercial graphene nanoplatelets. J Rheol (N Y N Y) 63:961–976. https://doi.org/10.1122/1.5108919

Hu K, Kulkarni DD, Choi I, Tsukruk VV (2014) Graphene-polymer nanocomposites for structural and functional applications. Prog Polym Sci 39:1934–1972. https://doi.org/10.1016/j.progpolymsci.2014.03.001

Hummers WS, Offeman RE (1958) Preparation of graphitic oxide. J Am Chem Soc 80:1339–1339. https://doi.org/10.1021/ja01539a017

Ivanov E, Velichkova H, Kotsilkova R et al (2017) Rheological behavior of graphene/epoxy nanodispersions. Appl Rheol 27. https://doi.org/10.3933/APPLRHEOL-27-24469

Jain S, Goossens JGP, Peters GWM, van Duin M, Lemstra PJ (2008) Strong decrease in viscosity of nanoparticle-filled polymer melts through selective adsorption. Soft Matter 4:1848–1854. https://doi.org/10.1039/b802905a

Kharchenko SB, Douglas JF, Obrzut J, Grulke EA, Migler KB (2004) Flow-induced properties of nanotube-filled polymer materials. Nat Mater 3:564–568. https://doi.org/10.1038/nmat1183

Kim H, Macosko CW (2009) Processing-property relationships of polycarbonate/graphene composites. Polymer (Guildf) 50:3797–3809. https://doi.org/10.1016/j.polymer.2009.05.038

Kim H, Miura Y, MacOsko CW (2010a) Graphene/polyurethane nanocomposites for improved gas barrier and electrical conductivity. Chem Mater 22:3441–3450. https://doi.org/10.1021/cm100477v

Kim J, Cote LJ, Kim F, Yuan W, Shull KR, Huang J (2010b) Graphene oxide sheets at interfaces. J Am Chem Soc 132:8180–8186. https://doi.org/10.1021/ja102777p

Kotsilkova R, Pissis P (2007) Thermoset nanocomposites for engineering applications. Smithers Rapra Technology

Kuilla T, Bhadra S, Yao DH, Kim NH, Bose S, Lee JH (2010) Recent advances in graphene based polymer composites. Prog Polym Sci 35:1350–1375. https://doi.org/10.1016/j.progpolymsci.2010.07.005

Lebaron PC, Wang Z, Pinnavaia TJ (1999) Polymer-layered silicate nanocomposites: an overview. Appl Clay Sci 15:11–29. https://doi.org/10.1016/S0169-1317(99)00017-4

Leblanc JL (2002) Rubber-filler interactions and rheological properties in filled compounds. Prog. Polym. Sci. 27:627–687

Leblanc JL (2009) Filled Polymers. CRC Press

Lerf A, He H, Forster M, Klinowski J (1998) Structure of graphite oxide revisited. J Phys Chem B 102:4477–4482. https://doi.org/10.1021/jp9731821

Li J, Ma PC, Chow WS, To CK, Tang BZ, Kim JK (2007) Correlations between percolation threshold, dispersion state, and aspect ratio of carbon nanotubes. Adv Funct Mater 17:3207–3215. https://doi.org/10.1002/adfm.200700065

Li D, Müller MB, Gilje S, Kaner RB, Wallace GG (2008) Processable aqueous dispersions of graphene nanosheets. Nat Nanotechnol 3: 101–105. https://doi.org/10.1038/nnano.2007.451

Liao KH, Qian Y, MacOsko CW (2012) Ultralow percolation graphene/polyurethane acrylate nanocomposites. Polymer (Guildf) 53:3756–3761. https://doi.org/10.1016/j.polymer.2012.06.020

Mackay ME, Dao TT, Tuteja A, Ho DL, van Horn B, Kim HC, Hawker CJ (2003) Nanoscale effects leading to non-einstein-like decrease in viscosity. Nat Mater 2:762–766. https://doi.org/10.1038/nmat999

Malkin AY (1990) Rheology of filled polymers. Adv Polym Sci 96:68–97. https://doi.org/10.1007/3-540-52791-5_2

Martinez CR, Iverson BL (2012) Rethinking the term "pi-stacking". Chem Sci 3:2191–2201. https://doi.org/10.1039/c2sc20045g

Mittal V (2014) Functional polymer nanocomposites with graphene: a review. Macromol Mater Eng 299:906–931. https://doi.org/10.1002/mame.201300394

Moraes LR d C, Ribeiro H, Cargnin E et al (2020) Rheology of graphene oxide suspended in yield stress fluid. J Nonnewton Fluid Mech 286: 104426. https://doi.org/10.1016/j.jnnfm.2020.104426

Munoz PAR, De Oliveira CFP, Amurin LG et al (2018) Novel improvement in processing of polymer nanocomposite based on 2D materials as fillers. eXPRESS Polym Lett 12:930–945. https://doi.org/10.3144/expresspolymlett.2018.79

Münstedt H (2016) Rheological and morphological properties of dispersed polymeric materials. Carl Hanser Verlag GmbH & Co. KG

Nakajima T, Matsuo Y (1994) Formation process and structure of graphite oxide. Carbon N Y 32:469–475. https://doi.org/10.1016/0008-6223(94)90168-6

Nan C-W, Shen Y, Ma J (2010) Physical properties of composites near percolation. Annu Rev Mater Res 40:131–151. https://doi.org/10.1146/annurev-matsci-070909-104529

Ng HC-H, Corker A, García-Tuñón E, Poole RJ (2020) GO CaBER: capillary breakup and steady-shear experiments on aqueous graphene oxide (GO) suspensions. J Rheol (N Y N Y) 64:81–93. https://doi.org/10.1122/1.5109016

Novoselov KS, Geim AK, Morozov SV, Jiang D, Zhang Y, Dubonos SV, Grigorieva IV, Firsov AA (2004) Electric field effect in atomically thin carbon films. Science 306:666–669. https://doi.org/10.1126/science.1102896

Pinto GM, Silva G d C, Santillo C et al (2020) Crystallization kinetics, structure, and rheological behavior of poly(ethylene terephthalate)/multilayer graphene oxide nanocomposites. Polym Eng Sci 60:2841–2851. https://doi.org/10.1002/pen.25516

Pötschke P, Fornes TD, Paul DR (2002) Rheological behavior of multiwalled carbon nanotube/polycarbonate composites. Polymer (Guildf) 43:3247–3255. https://doi.org/10.1016/S0032-3861(02)00151-9

Potts JR, Dreyer DR, Bielawski CW, Ruoff RS (2011) Graphene-based polymer nanocomposites. Polymer (Guildf) 52:5–25. https://doi.org/10.1016/j.polymer.2010.11.042

Saravanan N, Rajasekar R, Mahalakshmi S, Sathishkumar TP, Sasikumar KSK, Sahoo S (2014) Graphene and modified graphene-based polymer nanocomposites—a review. J Reinf Plast Compos 33:1158–1170. https://doi.org/10.1177/0731684414524847

Soares Y, Cargnin E, Naccache M, Andrade R (2020) Influence of oxidation degree of graphene oxide on the shear rheology of poly(ethylene glycol) suspensions. Fluids 5:41. https://doi.org/10.3390/fluids5020041

Song J, Yang W, Fu F, Zhang Y (2014) The effect of graphite on the water uptake, mechanical properties, morphology, and EMI shielding effectiveness of HDPE/Bamboo flour composites. BioResources 9:3955–3967. https://doi.org/10.15376/biores.9.3.3955-3967

Stankovich S, Dikin DA, Dommett GHB, Kohlhaas KM, Zimney EJ, Stach EA, Piner RD, Nguyen SBT, Ruoff RS (2006) Graphene-based composite materials. Nature 442:282–286. https://doi.org/10.1038/nature04969

Stankovich S, Dikin DA, Piner RD et al (2007) Synthesis of graphene-based nanosheets via chemical reduction of exfoliated graphite oxide. https://doi.org/10.1016/j.carbon.2007.02.034

Stauffer D, Aharony A, Aharony A (2014) Introduction to percolation theory. Taylor & Francis

Sternstein SS, Zhu AJ (2002) Reinforcement mechanism of nanofilled polymer melts as elucidated by nonlinear viscoelastic behavior. Macromolecules 35:7262–7273. https://doi.org/10.1021/ma020482u

Sun L, Boo W-J, Liu J, Clearfield A, Sue HJ, Verghese NE, Pham HQ, Bicerano J (2009) Effect of nanoplatelets on the rheological behavior of epoxy monomers. Macromol Mater Eng 294:103–113. https://doi.org/10.1002/mame.200800258

Takeh A, Shanbhag S (2013) A computer program to extract the continuous and discrete relaxation spectra from dynamic viscoelastic measurements. Appl Rheol 23:24628. https://doi.org/10.3933/ApplRheol-23-24628

Wagener R, Reisinger TJG (2003) A rheological method to compare the degree of exfoliation of nanocomposites. Polymer (Guildf) 44:7513–7518. https://doi.org/10.1016/j.polymer.2003.01.001

Wan C, Chen B (2012) Reinforcement and interphase of polymer/graphene oxide nanocomposites. J Mater Chem 22:3637. https://doi.org/10.1039/c2jm15062j

Wu G, Lin J, Zheng Q, Zhang M (2006) Correlation between percolation behavior of electricity and viscoelasticity for graphite filled high density polyethylene. Polymer (Guildf) 47:2442–2447. https://doi.org/10.1016/j.polymer.2006.02.017

Yang M, Koutsos V, Zaiser M (2005) Interactions between polymers and carbon nanotubes: a molecular dynamics study. J Phys Chem B 109:10009–10014. https://doi.org/10.1021/jp0442403

Zhang Q, Lippits DR, Rastogi S (2006) Dispersion and rheological aspects of SWNTs in ultrahigh molecular weight polyethylene. Macromolecules 39:658–666. https://doi.org/10.1021/ma051031n

Zhao J, Morgan AB, Harris JD (2005) Rheological characterization of polystyrene–clay nanocomposites to compare the degree of exfoliation and dispersion. Polymer (Guildf) 46:8641–8660. https://doi.org/10.1016/j.polymer.2005.04.038

Zhu Y, Murali S, Cai W, Li X, Suk JW, Potts JR, Ruoff RS (2010) Graphene and graphene oxide: synthesis, properties, and applications. Adv Mater 22:3906–3924. https://doi.org/10.1002/adma.201001068

Zouari R, Domenech T, Vergnes B, Peuvrel-Disdier E (2012) Time evolution of the structure of organoclay/polypropylene nanocomposites and application of the time-temperature superposition principle. J Rheol (N Y N Y) 56:725–742. https://doi.org/10.1122/1.4708602